ECCOMAS Congress 2016
VII European Congress on Computational Methods in Applied Sciences and Engineering
M. Papadrakakis, V. Papadopoulos, G. Stefanou, V. Plevris (eds.)
Crete Island, Greece, 5–10 June 2016

TOPOLOGY OPTIMIZATION USING A KRIGING-ASSISTED GENETIC ALGORITHM WITH A NOVEL LEVEL SET REPRESENTATION APPROACH

Mitsuo Yoshimura[1], Koji Shimoyama[1], Takashi Misaka[1], and Shigeru Obayashi[1]

[1] Institute of Fluid Science
Tohoku university
2-1-2 Katahira, Aoba-ku, Sendai, Japan
e-mail: {yoshimura, shimoyama, misaka, obayashi}@edge.ifs.tohoku.ac.jp

Keywords: Topology Optimization, Level-set Function, Computational Fluid Dynamics, Genetic Algorithm, Kriging Model.

Abstract. *Topology optimization is an optimization method which can modify connectivity of an object independently of its predefined topology. In this paper, a global optimization method for topology optimization of flow channels considering fluid and heat transfer using a genetic algorithm is presented. A genetic algorithm (GA) is assisted by the Kriging surrogate model to reduce computational cost required for function evaluation. In the present method, the boundary of a flow channel is represented by a level set function. Topology optimization seldom employs GA since topology optimization requires a large number of design variables for a high degree of freedom for shape and topology representation and GA is not effective to handle such a large scale problem. This paper presents a novel representation method to obtain the distribution of level set function with a reasonable number of design variables. The design variables are given at the scattered control points in the design domain, and the Helmholtz equation is solved in the entire domain. The proposed method is applied to a single-objective optimization problem to maximize heat transfer. As a result, GA found several flow channels, each of which has similar objective function values but with different topology. The result indicates that the objective function is a multi-modal function, which means that a method of population-based multipoint simultaneous exploration such as GA is essential for the present topology optimization problem. Considering minimizing pressure loss of a flow channel as the second objective function, the proposed method is applied to a multi-objective optimization problem. As a result, we confirm that the proposed representation method enables to represent flow channels that balance both objective functions and GA captures the trade-off between two objective functions.*

1 INTRODUCTION

Shape optimization has been attracting much attention in flow problems, which defines the boundary between fluid and solid regions. However, shape optimization cannot deal with the change of topology, *e.g.*, making new holes into an object. Topology optimization is the most flexible optimization method, which can modify connectivity of an object independently of its predefined topology in contrast to sizing optimization and shape optimization that keep their topology during the optimization.

Topology optimization has been applied to a variety of engineering optimization problems [1] such as structural mechanics problems [2], heat transfer problems [3], and acoustic problems [4] since Bendsøe and Kikuchi first proposed the so-called homogenization design method [5]. Although the topology optimization method for structural design has matured in the past few decades, the application to flow problems is still limited due to the non-linearity of the governing equations. The first application to flow problems was later than the aforementioned applications. It was performed for the Stokes flow by Borrvall and Petersson [6].

The basic concept of topology optimization is replacement of the optimization problem with a material distribution problem in a fixed design domain using a characteristic function that indicates whether material exists or not. However, conventional topology optimization tends to suffer from numerical instabilities such as checkerboard pattern [7]. The level set method [8-11] is one of the approaches to avoid such instabilities. The level set method introduces a signed scalar function called level set function and distinguishes solid and fluid regions according to the sign of the function. Thus, zero-contours of the function indicate the boundaries of the regions.

Topology optimization often contains a large design space due to a high degree of freedom for shape and topology representation (i.e., the number of design variables is often equal to the number of elements in the finite element mesh). Thus, conventional topology optimization generally has employed the gradient-based method according to the sensitivity of an objective function to explore the optimal solution and has been developed based on this approach. However, the gradient-based method tends to get stuck to the local optima rather than the global optimum. On the other hand, Evolutionary Algorithm (EA) such as Genetic Algorithm (GA) is one of the metaheuristic optimization methods, which is more capable to explore the global optimum. However, GA requires numerous function evaluations to realize population-based multipoint simultaneous exploration. Thus, GA is not efficient to solve the optimization problems with expensive calculations and requires much expensive computational cost (i.e., large population and many generations) to obtain competitive solutions. In this case, surrogate models are effective to reduce computational cost required for function evaluation. This model approximates the response of each objective or constraint function to design variables in an algebraic expression. This model is derived from several sample points with real values of the objective or constraint function given by expensive numerical simulations. Thus, it can promptly give estimates of function values at arbitrary design variable values.

The authors have proposed a non-gradient-based topology optimization method for single and multi-objective flow problems using GA assisted by the Kriging model [12]. Despite the results showed agreement with the results in previous studies [13] and revealed a novel insight into topology optimization problems, the representation method with the level set function obtained by solving a partial differential equation was not able to represent complex shapes. This study proposes a novel level set representation method using another partial differential equation. To validate the proposed representation method in a global topology optimization method applied to flow problems, this research focuses on a single-objective

optimization problems to maximize heat transfer, and a multi-objective optimization problem to minimize pressure loss and to maximize heat transfer of flow channels.

2 COMPUTATIONAL FORMULATIONS

Figure 1 shows a flowchart of the optimization process in this study. Details of each step in the flowchart are described as follows in this section. In Section 2.1 and 2.2, the representation method of flow channels and the Building-Cube Method (BCM), which is a Cartesian-mesh CFD approach to evaluate objective functions are stated. Section 2.3 presents NSGA II, a genetic algorithm employed in this study. Section 2.4 presents the Kriging model, a surrogate-model, and a criterion to decide additional sample points of the Kriging model.

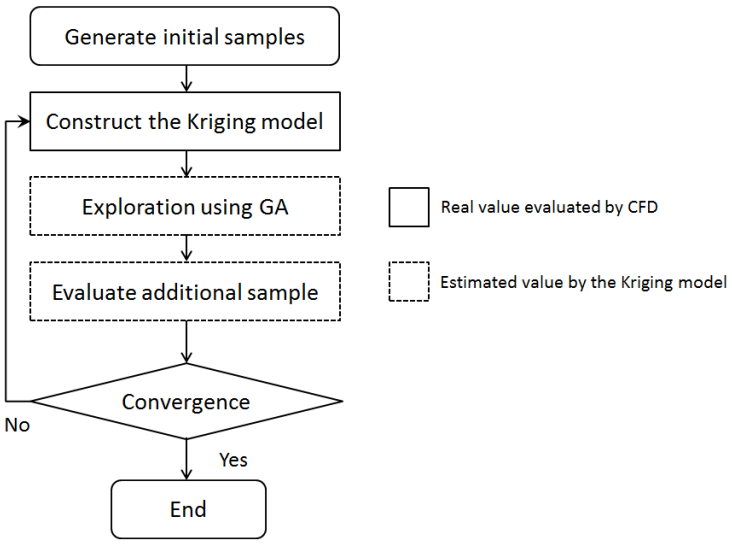

Figure 1: Optimization flowchart

2.1 Flow channel representation

In this section, a flow channel representation method proposed [12] and a novel method are stated. The boundaries between fluid and solid regions are represented by the level set representation that introduces a signed scalar function (level set function) $\phi(\boldsymbol{x})$ where $\boldsymbol{x}$ represents the location in the simulation domain. This research sets the range of $\phi(\boldsymbol{x})$ as $|\phi(\boldsymbol{x})| \leq 1$, and assumes $\boldsymbol{x}$ is in the fluid region if $\phi(\boldsymbol{x}) > 0$ or in the solid region if $\phi(\boldsymbol{x}) < 0$. A two-dimensional flow channel is described according to the sign of $\phi(\boldsymbol{x})$ given in the three-dimensional distribution. The example of the distribution of $\phi(\boldsymbol{x})$ is shown in Figure 2. As mentioned in Section 1, it is required to reduce the number of the design variables to employ GA for topology optimization. In this study, the distribution of $\phi(\boldsymbol{x})$ is obtained by several control points which are treated as the current design variables. Guirguis *et al.* employed a Kriging-interpolated level set (KLS) to obtain the distribution of $\phi(\boldsymbol{x})$ with a small number of the design variables and successfully applied GA to structural topology optimization [9]. The procedure to derive the distribution of $\phi(\boldsymbol{x})$ is stated below. First, at the outer boundary of the design domain, $\phi(\boldsymbol{x})$ is given as the step functions corresponding to the width of the inlet and outlet of the channel. Next, design variables ($\phi(\boldsymbol{x})$) are given at several discrete control points inside the design domain. Finally, the Laplace equation written in Eq. (1) is solved in the entire design domain to obtain the distribution of $\phi(\boldsymbol{x})$.

$$\frac{\partial^2 \phi}{\partial x^2} + \frac{\partial^2 \phi}{\partial y^2} = 0 \tag{1}$$

Note that the design variables are independent of the meshing size for CFD simulations in present method, which reduces the number of the design variables and enables the application of Genetic Algorithm for topology optimization problems.

The distribution of $\phi(\boldsymbol{x})$ derived from solving the Laplace equation is steep and several shapes cannot be represented by any value of $\phi(\boldsymbol{x})$ given at the control points as the design variables. For example, the channels whose boundary is exactly straight cannot be represented. This issue must be solved to compare the proposed method with the previous study whose results include straight wall boundaries. Thus, it is required to develop an advanced method which can alleviate the steep distribution smoother.

Thus, in order to tackle this issue, we introduce another step to derive smooth level set distribution. Inspired by a filtering method in [14], the Helmholtz equation written in Eq. (2) is introduced.

$$-\nabla\left[R_x \frac{\partial \varphi}{\partial x}, R_y \frac{\partial \varphi}{\partial y}\right]^T + \varphi(\boldsymbol{x}) = \phi(\boldsymbol{x}) \tag{2}$$

In Eq. (2), $\varphi(\boldsymbol{x})$ denotes a new distribution of level set function derived by solving the Helmholtz equation. $\phi(\boldsymbol{x})$, a solution of the Laplace equation, is substituted on the right hand side of Eq. (2). R_x and R_y are independent anisotropic weights of the Helmholtz equation that decide the alleviation strength of the level set distribution, $\phi(\boldsymbol{x})$. These weights are also involved as design variables and the present method enables to represent various shapes adaptively to the problems. Moreover, when both weights are set to 0, $\varphi(\boldsymbol{x})$ is identical to $\phi(\boldsymbol{x})$. This means that the present method provides a higher degree of freedom representation without sacrificing its original representation capability. It is important to note that although the flow channels evaluated by CFD simulation are represented based on the sign of $\varphi(\boldsymbol{x})$, the design variables considered in optimization are given at the control points in the $\phi(\boldsymbol{x})$ domain.

A conventional level set method for topology optimization [10, 11] employs the partial differential equation to update the value of level set function for a modified shape. The partial differential equation is solved with design sensitivities derived from the sensitivity analysis. In this study, on the other hand, the partial differential equation is not solved, and the value of $\phi(\boldsymbol{x})$ is updated based on the genetic algorithm stated in Section 2.3.

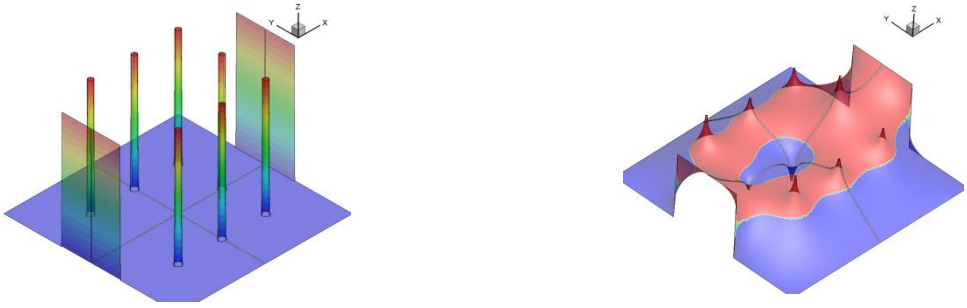

(a) Initial distribution (b) Final distribution

Figure 2: Distributions of the level set function obtained by solving the Laplace equation

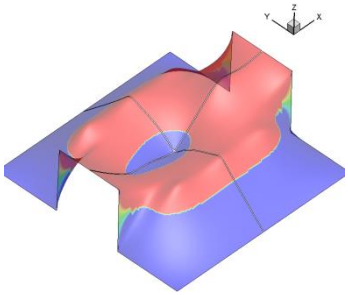

(a) 3D final distribution

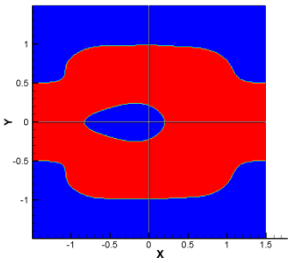

(b) 2D flow channel projected on the 2D design domain according to the sign of level set function of Figure 3 (a)

Figure 3: Distributions of the level set function obtained by solving theHelmholtz equation

2.2 Building-Cube Method

In order to evaluate the objective function of the channels, CFD simulations are conducted by the Building-Cube Method (BCM) [15], which is a Cartesian-mesh CFD approach. The governing equations of BCM are the 2D incompressible Navier-Stokes equations for unsteady state flow, and the 2D energy equation for unsteady state heat transfer. The convection terms are evaluated by a third-order upwind differencing [16], and the viscous terms are evaluated by a second-order central differencing. Time integration is conducted by the Crank-Nicolson method for the viscous terms and the Adams-Bashforth scheme for the convective terms, and the coupling of velocity and pressure is conducted by a fractional step method [17].

Since BCM employs a Cartesian-mesh CFD approach, it is easy to handle the complicated shapes of flow channels with topological change. However, in the Cartesian-mesh CFD approach, the object surface is represented by a staircase pattern, instead of smooth surface. For high accuracy computation, the Immersed Boundary Method (IBM) [18] using ghost cell and image point is employed at the wall boundary.

2.3 Genetic Algorithm

The genetic algorithm mimics the evolution of organisms, which selects individuals from the current generation as parents, generates new individuals as children by the crossover and mutation of the parents, and inherits better individuals to the next generation. In this study, the Non-dominated Sorting Genetic Algorithm II (NSGA-II) [19] proposed by Deb *et al.* is employed for exploration because this algorithm is effective and widespread employed for many optimization problems [9, 20]. Initially, a parent population $P_{t=1}$ with the size of N is created randomly. Here, t indicates the number of generation. Each feasible solution is assigned a rank (the solution with lower rank is better) according to its objective function value. On the other hand, each infeasible solution is assigned a rank which is higher than the minimum rank for the feasible solutions. Between two infeasible solutions, the solution with a smaller constraint violation has a better rank. Then, after choosing N solutions with lower rank in the parent population, recombination and mutation are conducted to create an offspring population Q_t with the size of N. In order to introduce elitism, first, a combined population $R_t = P_t \cup Q_t$ with the size of $2N$ is formed. Then, the solutions in R_t are sorted according to the ranks based on objective function values and constraint violation. Now, N solutions are chosen from R_t in the order of their ranks and make up a new population P_{t+1}. The procedure as described above

is for one generation. The non-dominated solutions with the lowest rank are explored by repeating this procedure for a certain number of generations.

2.4 Kriging model

Although GA is capable of finding the global optimum, it requires numerous function evaluations to realize population-based multipoint simultaneous exploration. For efficient global optimization, the Kriging surrogate model [21] is employed together with GA. The Kriging model is based on Bayesian statistics, and can adapt well to nonlinear functions. In addition, the Kriging model estimates not only the function values themselves but also their uncertainties. Based on these uncertainties, the expected improvement (EI) of an objective function, which may be achieved a new global optimum on the Kriging model by adding a new sample point, is estimated. In a single-objective optimization problem where $y(\boldsymbol{x})$ is minimized, the improvement value $I(\boldsymbol{x})$ and its expected value $E[I(\boldsymbol{x})]$ are defined as Eq. (3) and (4), respectively.

$$I(\boldsymbol{x}) = \begin{cases} [y_{min} - y] & \text{if } y < y_{min} \\ 0 & \text{otherwise} \end{cases} \tag{3}$$

$$E[I(\boldsymbol{x})] = \int_{-\infty}^{y_{min}} (y_{min} - y)\phi(y)dy \tag{4}$$

where ϕ is the probability density function denoted by $N[\hat{y}(\boldsymbol{x}), s^2(\boldsymbol{x})]$. Here, $\hat{y}(\boldsymbol{x})$ is the estimation of $y(\boldsymbol{x})$ and $s^2(\boldsymbol{x})$ is the mean square error at point $\boldsymbol{x}$ indicating the uncertainty of the estimated value. Maximizing the EI instead of the original objective function itself, the location of an additional sample point is determined for updating the Kriging model. Adding new samples to the Kriging model based on EI iteratively, these samples are expected to reach the global optima under the uncertainty of the Kriging model. This procedure is called Efficient Global Optimization (EGO) proposed by Jones *et al.* and widely employed for optimization [22].

Since the present optimization is capable of topological change, the flow channels may often become unconnected depending on design variable values. Since such unconnected channels make it difficult to evaluate the objective function values, they should not be considered as additional sample points for the Kriging model. Although GA has been successfully applied to topology optimization in several structural problems [9, 23, 24], it has not been accepted widely due in part to difficulty to ensure structural connectivity during the optimization procedure [25]. In order to ensure structural connectivity, the original EI value of the objective function, Eq. (4), is multiplied by the probability that the objective function value may be below a certain threshold estimated on the Kriging model. This probability $P(y(\boldsymbol{x}) < a)$, where a is a threshold, is formulated in

$$P(y(\boldsymbol{x}) < a) = \frac{1}{s\sqrt{2\pi}} \int_{-\infty}^{a} \exp\left(-\frac{(y(\boldsymbol{x}) - \hat{y}(\boldsymbol{x}))^2}{2s^2(\boldsymbol{x})} \right) dy \tag{5}$$

Maximizing the product of Eq. (4) and Eq. (5), the location of an additional sample point is determined for searching the global optima while assuring the connectivity of flow channels under the uncertainty of the Kriging model.

3 OPTIMIZATION PROBLEMS OF MAXIMIZING HEAT TRANSFER

In this section, two cases of the single-objective optimization to maximize heat transfer are presented. In this case, in addition to the 2D incompressible Navier-Stokes equation, the 2D

energy equation is also solved to evaluate the temperature field. In all case stated below, the design domain is discretized as a 240×240 uniform Cartesian grid. At the inlets, velocity is set as the Dirichlet boundary condition, parabolic profile given by Eq. (6) with the reference velocity of 1, and pressure is set as the Neumann condition.

$$g_n = \bar{g}\left(1 - (\frac{2s}{w})^2\right) \quad -\frac{w}{2} \le s \le \frac{w}{2} \tag{6}$$

where $\bar{g}$ is the prescribed velocity at the center of the flow profile, w is the width of the flow profile corresponding to the length of the inlet and the outlet, and s is location within the flow profile.

At the outlets, on the other hand, velocity is set as the Neumann condition and pressure is also set as the Dirichlet condition (zero pressure). Furthermore, no-slip boundary condition is given to the solid-fluid interface.

Temperature is set to be 0 at the inlet, and given by the Neumann condition at the outlet. Furthermore the temperature at the solid-fluid interface is expressed by the third type boundary condition as

$$-k\left(\frac{dT}{dx}\right)_{wall} = h(T_\infty - T_w) \tag{7}$$

where T_∞ is the temperature of the solid set to be 1, T_w is the fluid temperature on the wall, k and h correspond to the thermal conductivity and the heat transfer coefficient, respectively. In this study, h is given by the Nusselt number: $Nu = hl/k$. Here, the reference length l is the width of inlet set to be 1 and k is also set to be 1. Thus, the heat transfer coefficient is equal to the Nusselt number. The objective function is to maximize the bulk mean temperature T_m at the outlet given by

$$T_m = \frac{\int_{s_o} uTds}{\int_{s_o} uds} \tag{8}$$

where S_o indicates the area of the outlet, u and T are the velocity and the temperature at the outlet, respectively. In this problem, since the possible range of the objective function value is known thermodynamically (i.e., the maximum is not greater than the wall temperature: 1 and the minimum is not less than the inlet temperature: 0). Thus, this case does not introduce a threshold into the objective function value as seen in Eq. (5) because it can reduce the diversity of the population in GA. However, in order to ensure connectivity during the optimization and explore the global optimum efficiently, the product of the original EI value of the objective function, Eq. (4), is multiplied by the probability written in Eq. (5) that the objective function value may be above a certain value is maximized by GA. In this problem, the objective function is multiplied by -1 and to be minimized. The threshold a in Eq. (5) is set to be 0, which is the largest value of the objective function.

3.1 Single pipe (Case 1)

3.1.1. Problem definition

First, a single pipe illustrated in Figure 4(a) is considered. The Reynolds number and the Nusselt number are set to be 5 and 50, respectively. The Prandtl number is set to be 6.78. Each dimensionless number is chosen to compare the present study with the previous study [12, 26]. The layout of the control points are illustrated as red points in Figure 4(b). The de-

sign variables are given at the control points vertically symmetric in the range of [-1, 1] and the range of the weights for the Helmholtz equation is set to [0, 0.4]. Thus, the number of the design variables is 8 in Case 1. Since too large weights make the flow channels discontinuous, the valid range of the weights keeping the flow channel connected are investigated beforehand.

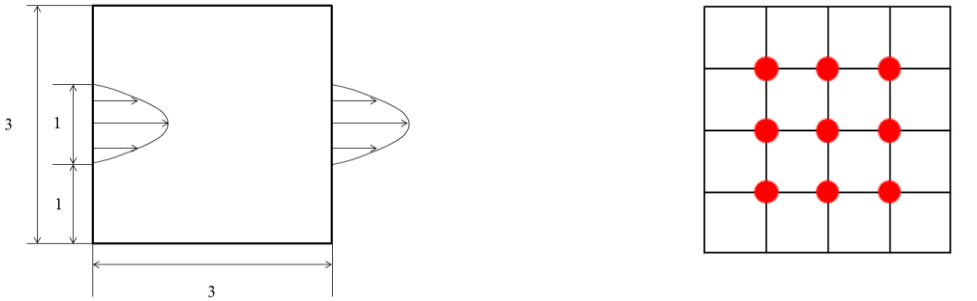

(a) Design domain (b) Layout of control points

Figure 4: Geometry definition of a single pipe (Cases 1)

3.1.2. Results

In this case, 218 initial sample points satisfying the connectivity from the inlet to the outlet are used to construct the Kriging model. The Kriging model is updated 18 times. Figure 5 shows representative flow channels in the additional samples. In this case, several flow channels, each of which has similar objective function values as shown in Table 1 but with different topology, are found as the local optima. This result indicates that the objective function is a multi-modal function and it is required to employ a method of population-based multipoint simultaneous exploration such as GA. The result also indicates that, as the number of the solid islands in the channels increases, the size of each island becomes smaller. This is because the size of island is determined by the length of solid-fluid interface to achieve an equal amount of heat flux on the interface.

Matsumori *et al.* pointed out that the current optimization problem is non-convex and has many local optima [27]. The present method confirms the same issue and copes with that by GA. GA finds several solutions as a local optimum with the same topology of the results reported in previous study [12]. Intuitively, large islands should be put to enhance fluid-thermal interaction. However, flow separation does not occur easily since this case employs low Reynolds number, and basically any shapes of large islands contribute high performance of heat transfer. Thus, the Helmholtz weights are small (i.e. a flow channel represented by solving the Laplace equation is acceptable as local optima directly) and the global optimum shown in Figure 5 (b) is very similar to the global optimum shown in Figure 5 (d) and reported in [12].

	Temperature
(a) 11th sample	0.8351
(b) 13th sample	0.8512
(c) 18th sample	0.8426

Table 1: Objective function values of the representative flow channels in the additional samples (Case 1).

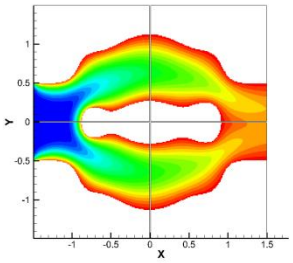

(a) 11th sample

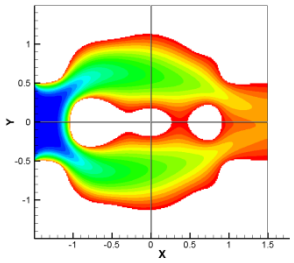

(b) 13th sample (global optimum)

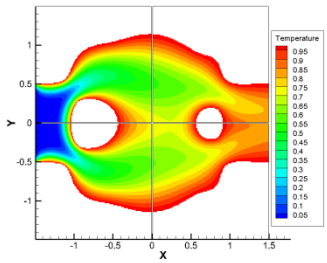

(c) 18th sample

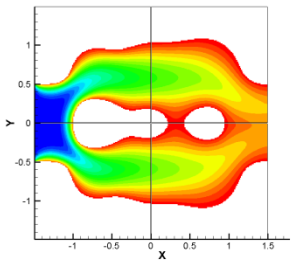

(d) The global optimum reported in [12]

Figure 5: Temperature distributions of the representative flow channels in the additional samples. (Case 1)

3.2 Double pipe (Case 2)

3.2.1. Problem definition

Second, a double pipe illustrated in Figure 6 (a) is considered. The Reynolds number and the Nusselt number are set to be 50 and 10, respectively. The layout of the control points are illustrated as red and blue points in Figure 6 (b). The design variables are given at the control points vertically symmetric in the ranges of [-1, 1] for red points and [0, 1] for blue points, and the range of the weights for the Helmholtz equation is set to [0, 0.4]. Thus, the number of the design variables is 20 in Case 2.

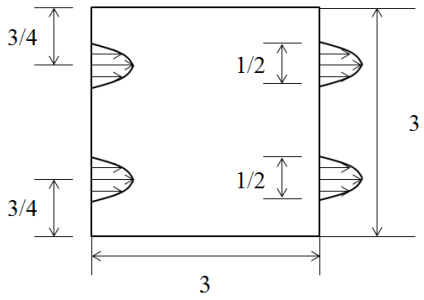

(a) Design domain

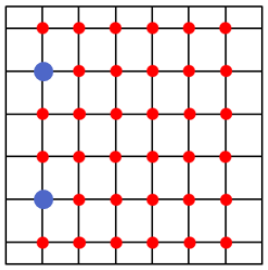

(b) Layout of control points

Figure 6: Geometry definition of a double pipe (Cases 2)

3.2.2. Results

In this case, 386 initial sample points satisfying the connectivity from the inlet to the outlet are used to construct the Kriging model. The Kriging model is updated 14 times. This case

has two differences from Case 1. First, since the Reynolds number in this case is higher than that in Case 1, flow separation occurs easily and several vortices are generated. Since these vortices affect heat transfer significantly, the shapes of islands inside the channels cannot be designed as arbitrarily as in Case 1. In Case 1, the flow channels with one or more islands have high temperature. In Case 2, on the other hand, putting islands arbitrarily does not always lead to high temperature. Second, since flow separation is a significant factor to increase temperature, the wall roughness and islands' shape are required to be smoothed by the Helmholtz weights whereas these weights are almost set to 0 in Case 1. It is important to note that the Helmholtz weights enable GA to explore efficiently because the design space is so complex that many details which do not contribute to the improvement of heat transfer are not removed during the optimization if the flow channels are represented only by the Laplace equation.

Figure 7 shows representative flow channels in the additional samples. Also in this case, several flow channels, each of which has similar objective function values but with different topology, are found as the local optima. However, in this case, as the number of islands increases, the objective function value also increases as shown in Table 2. In particular, the global optimum has much better objective function values compared with other local optima. As stated above, flow separation is a significant factor in a heat transfer problem, and we can confirm that the flow is not separated around the islands of the global optimum shown in Figure 7 (c). This result suggests that there is a dominant topology which shows high temperature. In this case, the present representation method always keeps the outer boundary of the flow channels smooth and lets GA explore efficient topology in the flow channels.

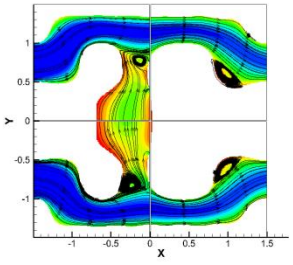

(a) 1st sample

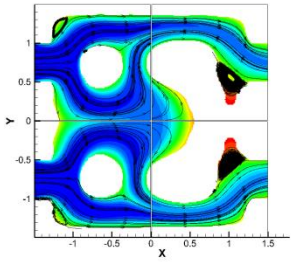

(b) 6th sample

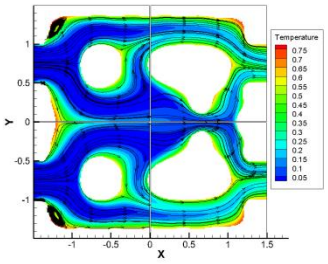

(c) 11th sample (global optimum)

Figure 7: Temperature distributions of the representative flow channels in the additional samples. (Case 2)

	Temperature
(a) 1st sample	0.1913
(b) 6th sample	0.2423
(c) 11th sample	0.2798

Table 2: Objective function values of the representative flow channels in the additional samples (Case 2).

4 MULTI-OBJECTIVE OPTIMIZATION PROBLEM

Finally, two cases of multi-objective optimization problem to minimize pressure loss and maximize heat transfer of flow channels are considered. Minimizing pressure loss Δp written in Eq. (9) is considered as the second objective function.

$$\Delta p = \left(\frac{1}{2}\rho u^2 + p\right)_{in} - \left(\frac{1}{2}\rho u^2 + p\right)_{out} \tag{9}$$

Two cases employ the same geometry of the design domain, velocity, pressure, temperature boundary conditions, and mesh resolution as Cases 1 and 2. Cases 3 and 4 employ the same combinations of dimensionless numbers as Cases 1 and 2, respectively.

There are a number of non-dominated solutions, which are not worse than any other solution regarding all objective functions, in a multi-objective optimization problem whereas there is only one optimal solution in a single-objective optimization problem. Thus, it is important to ensure the diversity of the solutions in GA and capture the trade-off among objective functions. Hence, it should be careful to introduce a threshold of the pressure loss while keeping the diversity of the solutions in GA. However, without a threshold, initial sample points including huge pressure loss are used to construct the Kriging model, which may make the estimation accuracy of the Kriging model worse. Since the width of those flow channels is very small, these flow channels can be regarded as unconnected. Moreover, the bulk mean temperature of such unconnected or nearly unconnected flow channels is evaluated to be 0 in Cases 1 and 2. Thus, such solutions are hardly able to be the non-dominated solutions, and it will not lose the diversity of solutions even if such solutions are removed from initial sample points. Multi-objective optimization employs several additional sample points every time the Kriging model is updated whereas a single-objective optimization employs one additional sample point for every update. This study performs cluster analysis using the k-means method [28] to select representative sample points from many non-dominated solutions obtained by maximizing the EI value of each objective function on the Kriging model. In both cases stated below, 4 additional sample points are chosen for every update.

4.1 Single pipe (Case 3)

4.1.1. Problem definition

As the first example, a single pipe illustrated in Figure 4 (a) is considered. This case employs the same dimensionless numbers and the layout of control points as Case 1.

4.1.2. Results

In this case, 275 initial sample points satisfying the connectivity from the inlet to the outlet are used to construct the Kriging model. In this case, a threshold of the pressure loss is introduced and set to be 20. Since the value range of the objective function of pressure loss is so wide that the log transformed pressure loss is approximated by the Kriging model whereas the temperature is approximated directly. Figure 8 plots of the initial sample points (blue), the non-dominated solutions obtained after the 19th update of the Kriging model using the present method (red), and the non-dominated solutions obtained after the 19th update reported in [12] (green) in the objective space. The non-dominated solutions in the 19th update can be classified into 3 groups according to their characteristics.

First, in the yellow group, the flow channels have low pressure loss and low bulk mean temperature. These flow channels do not include any solid island inside the channels.

Second, all solutions in the blue group have one island and all but one solutions in the purple group have one island in the channel. Thus, the solutions in these two groups have the same characteristic with respect to their topology whereas the solutions reported in the previous study [12] can be classified based on their topology (i.e. the number of the solid islands in a channel). We classify the solutions in the blue and purple group based on the shape of the island in the channel. The island of the solutions in the blue group is a small round or streamlined. On the other hand, the island of the solutions in the purple group is a large round or blunt body. As illustrated in Figure 8, the channel with a streamlined island can improve its temperature whereas the pressure loss does not increase drastically compared with the channel with a round island. Four solutions in the purple group have a weak trade-off between two objective functions; they have almost the same bulk mean temperature to the optimum found in Case 1 whereas the pressure loss gets larger in proportion to the size of the island. This result indicates that the bulk mean temperature reaches its upper limit thermodynamically in these 4 solutions. This result indicates that the heat transfer is saturated and the pressure loss increases monotonically at this point, that is, the blue group is important from an engineering standpoint.

Since this case employs very low Reynolds number, the effect of the streamlined island which is expected to prevent flow separation does not appear clearly and the non-dominated front itself is not improved compared with that of the previous study [12]. However, the streamlined shapes show their capability to improve heat transfer and prevent the pressure loss getting worse drastically. Thus, the present method is promising to solve the problems with complex flow phenomena such as flow separation and indicates the possibility of designing a flow channel satisfying both high temperature and low pressure loss.

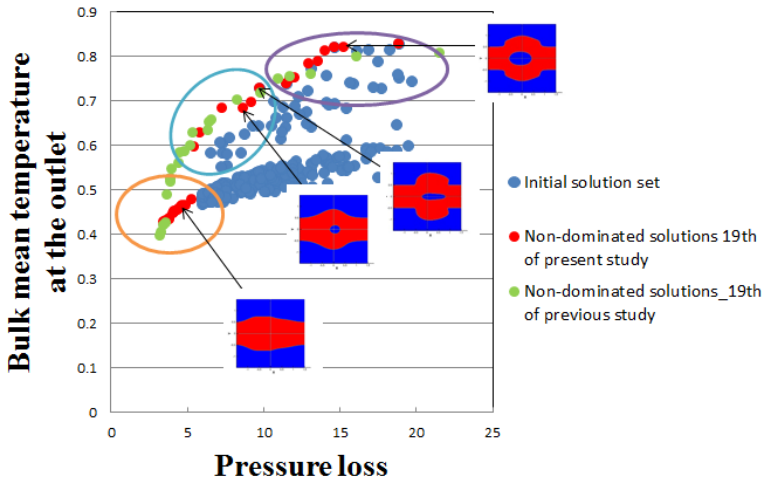

Figure 8: The solution set in the multi-objective problem (Case 3)

4.2 Double pipe (Case 4)

4.2.1. Problem definition

Finally, a multi-objective optimization problem of a double pipe illustrated in Figure 6 (a) is considered. This case employs the same dimensionless numbers and the layout of control points as Case 2.

4.2.2. Results

In this case, the initial sample points of the Kriging model are formed from 446 sample points satisfying the connectivity from the inlet to the outlet generated randomly and the global optimum of the single-objective optimization (Case 2). Hence, the number of the initial sample points is 447 in total. In this case, a threshold of the pressure loss is set to be 13. As well as Case 3, the log transformed pressure loss is approximated by the Kriging model whereas the temperature is approximated directly. Figure 9 plots the initial sample points (blue), the non-dominated solutions obtained after the 10^{th} update of the Kriging model with the global optimum in the initial sample points (green), and the non-dominated solutions obtained after the 11^{th} update without the global optimum in the initial sample points (red) in the objective space. As Figure 9 shows, the global optimum of the single-objective optimization facilitates GA to explore the non-dominated solutions that balance two objective functions.

In this case, low pressure loss can be achieved easily. As stated in Case 2, if the flow does not separate from an island put in a channel, the heat transfer performance does not worsen severely. It is obvious that the pressure loss gets larger if the flow separates in the channel. Thus, we anticipate that we can design a flow channel balancing both objective functions if the islands put in a channel can avoid flow separation. As shown in Figure 9, the red solutions (they are dominated solutions inherently since the true non-dominated solutions are green points) show improvement on heat transfer depending on the shape of the solid-fluid interface. Comparing two red solutions in Figure 9, we find that the backward shape of the left one is convex so that it can prevent flow separation whereas the backward of right one is flat. Thus, the left solution can balance two objective function whereas the pressure loss of the right one becomes larger despite its temperature is high since the solid-fluid interface is longer than that of the left one. However, as the green points in the blue circle indicate, two objective functions can be more improved if the backward is separated into two isolated islands. Flow separation does not occur in all of the green solutions and the values of the objective functions depend on the sizes of the backward islands; starting from ellipses (low pressure loss and low temperature), the backward islands become larger and transform into the same shape with the global optimum of the single-objective optimization in the channel with the highest temperature.

Thus, the proposed representation method enables to represent various shapes that contribute to improve both objective functions concurrently and GA reveals a dominant topology satisfying both objective functions.

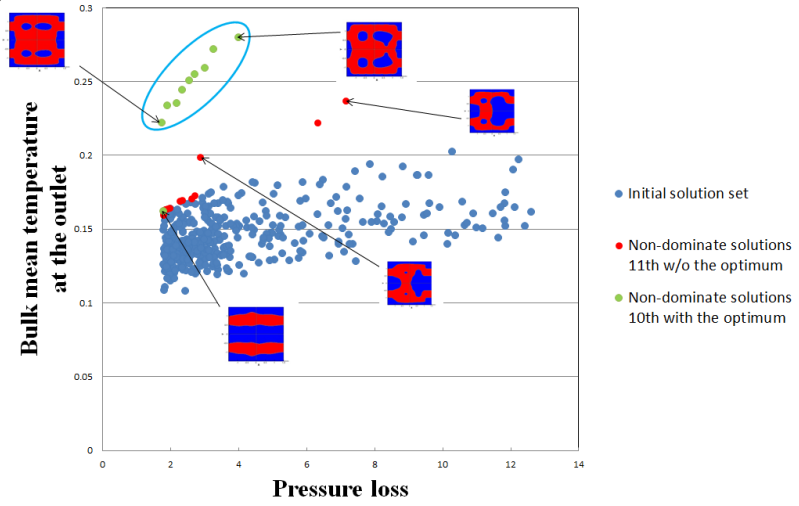

Figure 9: The solution set in the multi-objective problem (Case 4)

5 CONCLUSIONS

Topology optimization employing a Kriging-assisted GA was conducted in flow channel design problems that maximize heat transfer and/or minimize pressure loss using a novel level set representation approach.

In the single-objective optimization problems to maximize the bulk mean temperature, two cases with different layouts and dimensionless numbers were conducted. The GA found not only the optimal shape, but also several shapes that have quite similar objective function values but with different topologies from each other. In both cases, the objective function of temperature seems to be a multi-modal function and putting a solid island in a fluid region and increasing the length of the solid-fluid interface have significant effects to increase the temperature. However, in the case at the high Reynolds number, the flow separation severely affects heat transfer performance and the shape of islands should be considered so as not to provoke flow separation. The proposed representation method was able to represent various shapes which improve heat transfer and facilitated efficient exploration of GA in the complex design space.

Finally, considering minimizing pressure loss as the second objective function, multi-objective optimization problems were conducted in the same layout and numerical conditions with those of each case in the single-objective optimization problems. As a result, it was revealed that the size and the shape of a solid island put in a flow channel are the most important factors to increase the temperature and determine the pressure loss for both cases. Because the proposed representation method is able to represent streamlined shape, we could design flow channels with relatively large island without flow separation. Those flow channels with streamlined island were found as non-dominated solutions by GA. These solutions indicate that the proposed representation method is expected to help us design the flow channels that satisfy high temperature and low pressure loss at the same time.

Therefore, the proposed representation method and heuristic approach showed its capability to design promising flow channels and to explore global optima for both single-objective and multi-objective topology optimization in flow problems more efficiently.

REFERENCES

[1] M.P. Bendsøe, O. Sigmund, *Topology optimization: theory, methods and applications*, Springer, 2003.

[2] G.I.N. Rozvany, Aims, scope, methods, history and unified terminology of computer-aided topology optimization in structural mechanics. *Structural and Multidisciplinary Optimization*, **21**(2), 90-108, 2001.

[3] E.M. Dede, Multiphysics topology optimization of heat transfer and fluid flow systems. *proceedings of the COMSOL Users Conference* 2009.

[4] M.B. Dühring, J.S. Jensen, O. Sigmund, Acoustic design by topology optimization. *Journal of sound and vibration*, **317**(3), 557-575, 2008.

[5] M.P. Bendsøe, N. Kikuchi, Generating optimal topologies in structural design using a homogenization method. *Computer Methods in Applied Mechanics and Engineering*, **71**(2), 197-224, 1988.

[6] T. Borrvall, J. Petersson, Topology optimization of fluids in Stokes flow. *International Journal for Numerical Methods in Fluids*, **41**(1), 77-107 2003.

[7] O. Sigmund, J. Petersson, Numerical instabilities in topology optimization: a survey on procedures dealing with checkerboards, mesh-dependencies and local minima. *Structural optimization*, **16**(1), 68-75, 1998.

[8] J.A. Sethian, A. Wiegmann, Structural Boundary Design via Level Set and Immersed Interface Methods. *Journal of Computational Physics*, **163**(2), 489-528, 2000.

[9] D. Guirguis, K. Hamza, M. Aly, H. Hegazi, K. Saitou, Multi-objective topology optimization of multi-component continuum structures via a Kriging-interpolated level set approach. *Structural and Multidisciplinary Optimization*, **51**(3), 733-748, 2015.

[10] G. Allaire, F. Jouve, A.M. Toader, Structural optimization using sensitivity analysis and a level-set method. *Journal of Computational Physics*, **194**(1), 363-393, 2004.

[11] S. Yamasaki, T. Nomura, A. Kawamoto, K. Sato, S. Nishiwaki. A level set-based topology optimization method targeting metallic waveguide design problems. *International Journal for Numerical Methods in Engineering*, **87**(9), 844-868, 2011.

[12] M. Yoshimura, T. Misaka, K. Shimoyama, S. Obayashi, Topology optimization of flow channels with heat transfer using a genetic algorithm assisted by the Kriging model. *EUROGEN 2015*, Glasgow, UK, Sept 14-16, 2015.

[13] V.J. Challis, J.K. Guest, Level set topology optimization of fluids in Stokes flow. *International Journal for Numerical Methods in Engineering*, **79**(10), 1284-1308, 2009.

[14] B.S Lazarov, O. Sigmund, Filters in topology optimization based on Helmholtz-type differential equations. *International Journal for Numerical Methods in Engineering*, **86**(6), 765-781, 2011.

[15] K. Nakahashi, L.S. Kim. Building-Cube Method for Large-Scale, High Resolution Flow Computations. *AIAA paper*, 2004-0423, 2004.

[16] T. Kawamura, K. Kuwahara, Computation of High Reynolds number Flow around Circular Cylinder with Surface Roughness. *AIAA paper,* 84-0340, 1984.

[17] J. Kim, P. Moin, Application of a Fractional-Step Method to Incompressible Navier-Stokes Equations. *Journal of Computational Physics*, **59**, 308-323, 1985.

[18] R. Mittal, H. Dong, M. Bozkurttas, F.M. Najjar, A. Vargas, A. von Loebbecke. A versatile sharp interface immersed boundary method for incompressible flows with complex boundaries. *Journal of Computational Physics*, **227**(10), 4825-4852, 2008.

[19] K. Deb, A. Pratap, S. Agarwal, T. Meyarivan, A fast and elitist multiobjective genetic algorithm: NSGAII. *Evolutionary Computation, IEEE Transactions*, **6**(2), 182–197, 2002.

[20] J.N. Richardson, F.C. Rajan, A. Sigrid, Robust topology optimization of truss structures with random loading and material properties: A multiobjective perspective. *Computers & Structures*, **154**, 41-47, 2015.

[21] D.R. Jones, M. Schonlau, W.J. Welch, Efficient global optimization of expensive black-box functions. *Journal of Global Optimization*, **13**(4), 455–492, 1998.

[22] F.A.C. Viana, T.W. Simpson, V. Balabonov, V. Toropov. Metamodeling in Multidisciplinary Design Optimization: How Far Have We Really Come?. *AIAA Journal*, **52**(4), 670-690, 2014.

[23] S.Y. Wang, K. Tai, M.Y. Wang, An enhanced genetic algorithm for structural topology optimization. *International Journal for Numerical Methods in Engineering*, **65**(1), 18-44, 2006.

[24] J.K. Guest, L.C. Smith Genut, Reducing dimensionality in topology optimization using adaptive design variable fields. *International Journal for Numerical Methods in Engineering*, **81**(8), 1019-1045, 2010.

[25] J.D. Deaton, R.V. Grandhi, A survey of structural and multidisciplinary continuum topology optimization: post 2000. *Structural and Multidisciplinary Optimization*, **49**(1), 1-38, 2014.

[26] T. Matsumori, T. Kondoh, A. Kawamoto, T. Nomura, Flow channel design in heat exchanger for maximum heat transfer by topology optimization. *Proceedings of 20th Design & Systems Conference*, 3103.1-4, 2010. (in Japanese)

[27] T. Matsumori, T. Kondoh, A. Kawamoto, T. Nomura, Topology optimization for fluid-thermal interaction problems under constant input power. *Structural and Multidisciplinary Optimization*, **47**(4), 571-581, 2013.

[28] A.K. Jain, M.N. Murty, P.J. Flynn, Data clustering: a review. *ACM computing surveys (CSUR)*, **31**(3), 264-323, 1999.